SHEAR BEHAVIOR OF REINFORCED HIGH-STRENGTH CONCRETE MEMBERS

Saitama University, Japan　○ Perera, S.V.T.J.
Saitama University, Japan　JPCEA Member, Mutsuyoshi, H.

Abstract: This paper describes the diagonal cracking shear behavior of reinforced high-strength concrete (HSC) members without web reinforcement. It was found that the diagonal cracking shear strength of HSC is governed by the ratio of uniaxial compressive strength to tensile strength (the ductility number, *DN*) of the concrete relative to that of the aggregate. As the *DN* of concrete exceeded that of the aggregate, diagonal cracking shear strength decreased due to the smooth fracture surface and brittleness.

Keywords: brittleness, ductility number, fracture surface, high-strength concrete, shear.

1. INTRODUCTION

Prestressed concrete (PC) is one of the most reliable, durable, and widely used construction materials in bridge constructions around the world. In a PC member, the concrete is pre-compressed before it is placed in use. As loads are applied, the areas of the structure which would normally go into tension simply lose some of their pre-compression. In this manner, concrete is made to function in either tension or compression. Presently, PC is composed of high-strength concrete (HSC) and high-strength prestressing steel strands.

HSC with a strength, f'_c, exceeding 60 MPa is being increasingly used in buildings and PC bridges in Japan because it enables the use of smaller cross-sections, longer spans, and reduced girder height while improving durability [1]. The design shear capacity of a PC member is equal to the summation of diagonal cracking shear strength of members without web reinforcement, shear strength of web reinforcement and component of effective tensile force in longitudinal tendon [1]. However, the use of HSC has led to some concerns about its diagonal cracking shear strength since the shear strength does not increase as expected with the increase in the compressive strength of concrete [2, 3].

Diagonal cracking shear failure of RC members without web reinforcement initiates when the principal tensile stress within the shear span exceeds the tensile strength of concrete. Also, the diagonal cracking shear strength of a reinforced concrete (RC) member without web reinforcement is carried by the shear resistance of uncracked concrete in the compression zone, the interlocking action of aggregate (crushed and screened rock) along the concrete surfaces on each side of a crack, and the dowel action of the longitudinal reinforcement. In rectangular beams, the proportions of the shear strength carried by these mechanisms are as follows: 53-90% by the uncracked concrete in the compression zone and through aggregate interlocking, and 15-25% by dowel action [5]. That is, in RC beams without web reinforcement the shear force is mainly carried by the interlocking action of aggregate across flexural cracks and uncracked concrete in the compression zone. Both these mechanisms are dependent on concrete strength. Therefore, the diagonal cracking shear strength of RC members strongly depends on the strengths (compressive strength and tensile strength) of concrete. Also, the strengths of the aggregate control the strengths of concrete, particularly HSC. However, a fundamental theory explaining the diagonal cracking shear strength of beams relative to aggregate strengths is still missing.

In NSC, the properties of coarse-aggregate seldom become strength-limiting, since NSC mixtures typically correspond to water-cement ratios (w/c) in the order of 0.4 to 0.7. Within this w/c range, the weakest components in concrete are the hardened cement paste and the transition zone between the cement paste and coarse-aggregate, rather than coarse-aggregate itself [6]. However, in HSC, the hardened cement paste and the transition zone are no longer strength-limiting. This is because the concrete mixtures are usually made with a low w/c (0.2 to 0.3). On the contrary, it is the strength of the coarse-aggregate itself that controls the strength of HSC [3]. However, there is little information on the influence of coarse-aggregate characteristics on HSC strengths [7].

The fracture surface of HSC is relatively smoother than that of NSC since cracks penetrate through aggregate [8]. The effectiveness of shear transfer through aggregate interlock is commonly believed to be reduced if the coarse aggregate fractures at cracks as is frequently the case in HSCs. Until now, no theory has attempted to explain the roughness of concrete fracture surface relative to strengths of concrete and aggregate [3, 4]. It has been found that, the shear resistance of uncracked concrete in the compression zone is lower with HSC as a result of its brittleness [9].

Against this background, the objectives of this study are: 1) to quantitatively explain the effect of both concrete strength and aggregate strength on fracture surface of concrete, 2) to propose a diagonal cracking shear behavior with respect to aggregate and concrete strengths, and 3) to define the concrete strength regions.

2. DUCTILITY NUMBER (DN)

The effectiveness of shear transfer through aggregate interlock is believed to be reduced if the coarse aggregate fractures at cracks [3, 4]. Therefore, an understanding of the fracture mechanism of rock is a prerequisite for designing RC members. In fact, the study of brittle fracture forms is a fundamental research area in rock mechanics. The envelope for brittle failure is mainly determined by the peak stresses of the rock and can be determined using the Brazilian splitting tension test and uniaxial compression test [10]. Mohr's theory is often used to predict the failure of brittle materials. Therefore, the failure of rock is mostly described using Mohr's failure theory. In this study, linear Mohr's envelopes tangent to the Brazilian splitting tension tests and uniaxial compression tests were considered due to their easy application (Fig.1).

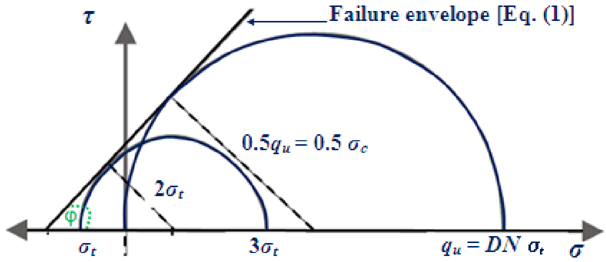

Fig.1 Mohr's failure envelope for Brazilian splitting tension test and uniaxial compression test

According to Fig.1, the failure envelope to the Brazilian tension circle and uniaxial compression circle can be expressed as follows

$$\tau = \left[\frac{(DN-4)}{2\sqrt{DN-3}}\right]\sigma + \frac{q_u}{2\sqrt{DN-3}} \qquad (1)$$

where, τ is shear stress, σ is normal stress, q_u is compressive strength, and *DN* is the ductility number [that is, the ratio of uniaxial compressive strength (σ_c) to tensile strength (σ_t)].

The value of *DN* can be used as a measure of material brittleness since it governs the material friction angle (φ) [11, 12]. Therefore, for a particular aggregate type, the value of *DN* can be used as a measure of concrete brittleness [3, 11, 12]. A higher value of *DN* corresponds to a more brittle concrete [3]. Also, when Mohr's circles of HSC strengths reach the rupture envelope of aggregate, aggregate in HSC ruptures resulting in a smooth fracture surface. That is, the *DN* of concrete (*DNC*) is higher than that of aggregate. The smooth crack surface reduced aggregate interlock and lowered the shear strength of HSC members. However, this behavior should be experimentally verified.

3. TEST PROGRAMS

3.1 Materials

In this study, the diagonal cracking shear behavior was described using the *DN*s of concrete and aggregate. As tabulated in Table 1, twelve beams without web reinforcement were used in this study. The cross sections and layout of test beams are shown in Fig.2. The test variables were compressive strength of concrete and shear span to effective depth (*a/d*) ratio.

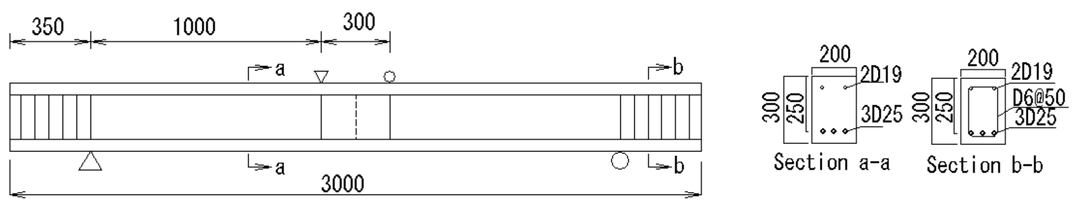

Fig.2 Details of RC beam (unit: mm)

All specimens including RC beams, compressive strength specimens (*Φ*100x200mm), and splitting tensile strength specimens (*Φ*150x300mm), were cured up to the loading test age to exclude the drying effects.

To determine the aggregate strengths, uniaxial compressive strength and tensile strength tests of rock cylinders were measured. Cylinder specimens measuring 50 mm in diameter and 100 mm in height were prepared for uniaxial compressive strength tests and others measuring 50mm in diameter and 50 mm in height were prepared for tensile strength tests (measured using the Brazilian test). Refer to Table 2 for the results of these tests.

3.2 Instrumentation and Measurements

The four-point symmetrical loading with a distance of 300 mm between the loading points was statically applied to all specimens (Fig.2). Vertical deflections at the center, shear span and support of the RC beam were measured by displacement transducers. The test was stopped when the crushing of the concrete in compression and considerable loss of load carrying capacity was observed.

A laser-light confocal microscope was used to scan the fractured splitting-tensile-strength test specimens' surface three dimensionally [3, 4]. A 100mmx100mm (at the center of the specimen) area of fractured surface was scanned with a 250μm pixel size and resolution of 0.01μm.

The interlocking action of aggregate along a crack can be described using post-failure evidence from the fracture surface. It is commonly recognized that the roughness of the fracture surface can vary depending on concrete mix design. Until now, however, this has not been quantitatively explained [3, 4].

For the surface roughness test, fractured splitting-tensile-strength test specimens were tested. The fracture surfaces of these specimens were not damaged since they failed in mode I. The roughness index (R_s) was calculated from the directly measured surface area [3, 4] as shown by Eq. (2) (Fig.3).

$$R_s = \frac{\text{actual surface area}}{\text{projected surface area}} = \frac{\Sigma Ai}{\Sigma \underline{A}} \qquad (2)$$

4. RESULTS AND DISCUSSION

4.1 Properties of Concrete

The compressive strength and splitting tensile strength at the time of the beam test are tabulated in Table 1. The roughness index, R_s, of the fracture surface is described using the *DN*. According to Table 2 and Fig.4 (a), the aggregate type (crushed granite) used in this study has a *DN* in the region of 18-22 due to the strength anisotropy of individual rocks [13, 14]. Therefore, the two strength measures (σ_c, σ_t) have maximum and minimum values that depend on the orientation of planes in the rock. Also, regarding the maximum and minimum values of *DN*, the maximum value is more critical because of brittleness [Eq. (1), Fig.4 (a)] [3, 4].

According to Fig.4 (a), the *DN* of aggregate (*DNA*) at the critical rupture envelope was 21.3. Fig.4 (b) explains how the fracture surfaces of HSC became smooth: Mohr's circles of concrete strengths are moving closer to the aggregate rupture envelope with an increasing *DN*. When Mohr's circle of NSC strengths [Fig.4 (a) f'_c=38 MPa] was under the rupture envelope of aggregate, the weakest components were the hardened cement paste and the transition zone between the cement paste and coarse aggregate rather than the strength of coarse aggregate. That is, the fracture surface was rough as cracks were not penetrated through aggregate [Fig.5 (a)]. However, when Mohr's circles of HSC strengths [Fig.4 (b) f'_c=183 MPa) reached the rupture envelope of aggregate, the weakest components was the strength of coarse aggregate. Therefore, aggregate in HSC ruptured with a smooth fracture surface. That is, the fracture surface of HSC was relatively smoother than that of NSC since cracks penetrate through aggregate (Fig.5).

Briefly, the DN of the aggregate relative to that of concrete governs the fracture surface roughness and brittleness of concrete. Mohr's circles of concrete strengths approach the aggregate rupture envelope as the *DN* increases. When Mohr's circles of HSC strengths pass the rupture envelope of the aggregate (*DNC*>*DNA*), the aggregate in HSC ruptures resulting in a smooth fracture surface (Fig.6). There was a 14% reduction in R_s between concrete with a strength of 36 MPa and 114 MPa (Fig. 6). However, as concrete strength further increased from 114 MPa to 155 MPa, the change in R_s was minimal (Fig. 6) (*DNC*≈*DNA*). This fracture surface roughness was due to the strength anisotropy of aggregate [Fig.4 (a)]. Also, the value of R_s of HA160-d concrete with a strength of 175 MPa was the same as that of HA150 concrete with a strength of 155 MPa concrete and it was minimal due to smooth fracture surface (Fig. 6). The smooth crack surface reduced aggregate interlock and lowered the shear strength of HSC (Fig.6 and Table 1). Further, friction angle [function of *DN*, Eq. (1)] of concrete was increased with the increase of concrete strength. Therefore, concrete brittleness also increased with the increase of concrete *DN* and led to reduced shear resistance in the uncracked compression zone of HSC (Table 1).

Table 1 Test variables and beam test results

Specimen	a/d	f'_c (MPa)	f_t (MPa)	V_c (kN)
NSC40-a	3.0	38	3.2	75.0
NSC40-b	3.5	38	3.4	78.0
NSC40-c	4.0	36	3.1	76.5
HA80	-	81	4.9	-
HA100-a	3.0	133	6.1	85.5
HA100-b	3.5	116	5.4	85.0
HA100-c	4.0	114	5.2	85.0
HA120	4.0	138	7.2	82.5
HA150	4.0	155	8.3	85.0
HA160-a	3.0	165	7.4	81.0
HA160-b	3.5	194	6.8	77.0
HA160-c	4.0	183	7.4	75.0
HA160-d	4.0	175	8.5	67.0

a/d: Shear span to depth ratio
f'_c: Compressive strength, f_t: Tensile strength
V_c: Shear force at diagonal cracking.

Table 2 Properties of aggregate

Type	σ_c (MPa)	σ_t (MPa)	Maximum aggregate size
Crushed granite	190-285	8.9-15.3	19 mm

σ_c: Uniaxial compressive strength
σ_t: Tensile strength (measured by Brazilian test)

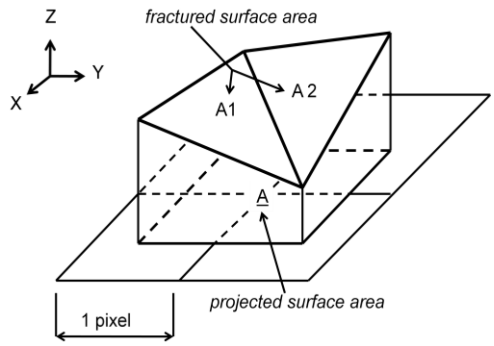

Fig.3 Schematic view of roughness parameter

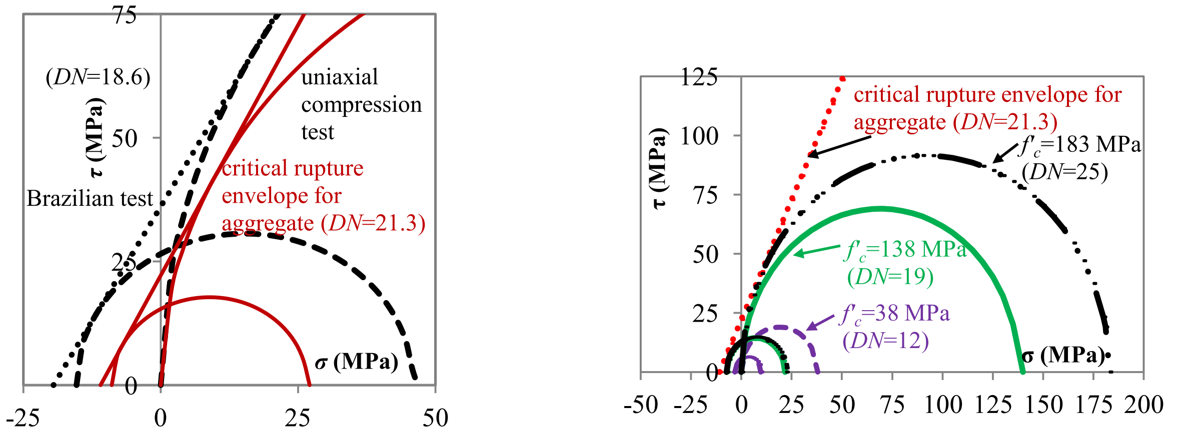

(a) Mohr's circles for rock strengths　　(b) Mohr's circles for different strengths of concrete

Fig.4 Mohr's circles for rock and concrete

4.2 Load-Deflection Relationship

Fig.7 shows the load-deflection curves of tested beams with a/d = 4.0. All beams exhibit similar behavior and beam HA160-c is described here as an example. In the HA160-c load-deflection curve, flexural cracks first appeared at an early stage of loading. The load dropped slightly after formation of the first flexural crack, and then continued to rise.

The diagonal crack then occurred in the shear span and the load dropped sharply. However, the load soon continued to increase, dropping slightly once again with the formation of another crack. Thus, even though diagonal cracking took place, the beam was still able to bear the applied load through arch action. Finally the beam failed in shear compression when the diagonal cracks in the shear span widened and the concrete near the crack tip in the compression zone was crushed. Beams HA100-a, HA100-b, HA150, HA160-a, HA160-b, HA160-c, and HA160-d all failed in shear compression while all other beams, including HA120 and HA100-c, failed in diagonal tension. Diagonal tension failure occurred just after the occurrence of critical diagonal cracking.

4.3 Diagonal Cracking Shear Behavior

Test results indicated that diagonal cracking shear strength of the HSC beam with a concrete strength of 114 MPa (beam HA100-c) was 11% higher than that beam in NSC40-c (f'_c 36 MPa). This increase was due to the roughness of the fracture surface (*DNC*<*DNA*) and the 67% increase in f_t. The shear strength of HSC beams was constant for concrete strengths between 114 MPa (beam HA100-c) and 155 MPa (beam HA150). This behavior was due to the improved f_t and the *DN* of the concrete and aggregate being approximately equal (Fig. 6 and Fig. 8) (*DNC*≈*DNA*). However, the shear strength of beam HA160-c (f'_c = 183 MPa) was 12% lower than that of beam HA150 (f'_c = 155 MPa) (Fig.8). This reduction was due to the smooth fracture surface (Fig. 6) and the increase in brittleness (*DNC*>*DNA*).

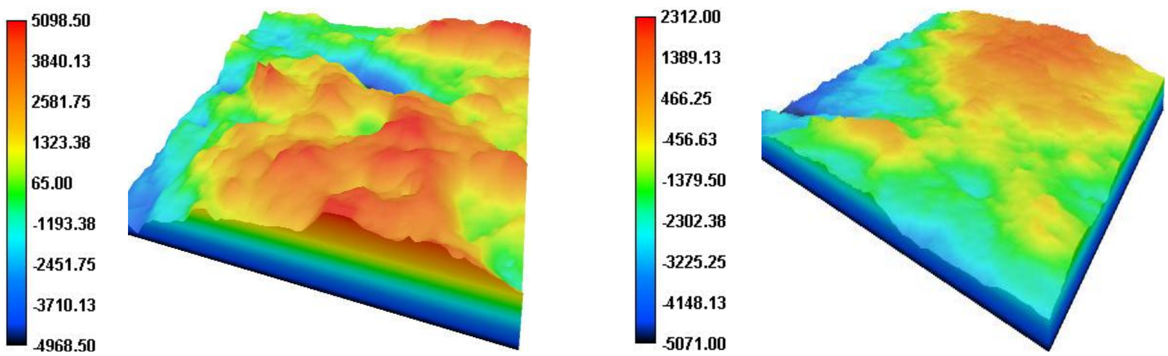

(a) f'_c = 36 MPa, R_s=1.269　　(b) f'_c = 183 MPa, R_s=1.047

Fig.5 Fracture surface of splitting-tensile-strength test specimens, R_S: surface roughness index (color code represent the surface elevation (µm))

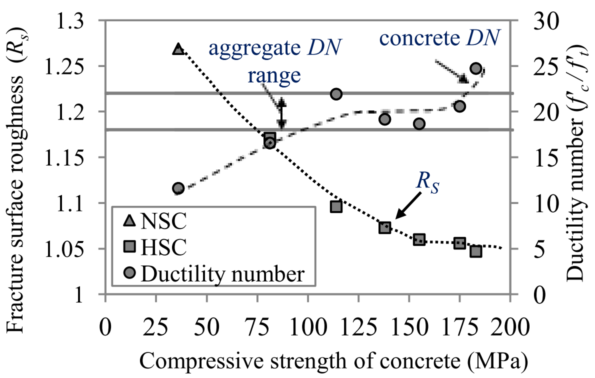

Fig.6 Fracture surface roughness of splitting-tensile-strength specimens

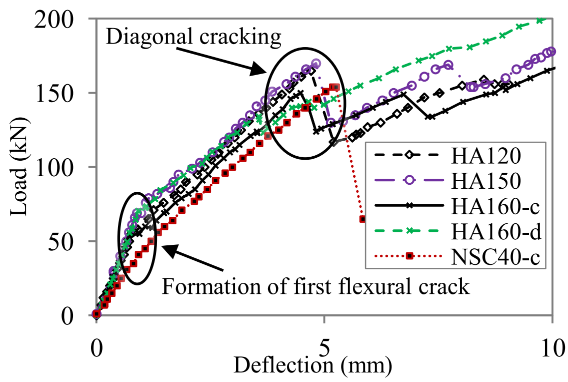

Fig.7 Comparison of load-deflection relationship of RC beams

4.4 Proposed Diagonal Cracking Shear Behavior

The *DN* of the concrete relative to that of the coarse aggregate governs the fracture surface roughness and brittleness of concrete and diagonal cracking shear strength of HSC. When the *DN* of concrete was lower than that of the aggregate, the shear strength increased with the increase of concrete strength due to rough fracture surface and increased tensile strength. When the *DN*s of the concrete and aggregate were equal, shear strength stayed constant at the maximum value. However, when concrete had a higher *DN* than the aggregate, shear strength decreased due to the smooth fracture surface and high brittleness of the concrete (Fig.9).

5. CONCLUSIONS

The shear behavior of RC beams without web reinforcement was investigated. The results of a series of tests on 12 beams were presented and analyzed.

The ductility number of the aggregate relative to that of concrete governs the fracture surface roughness of concrete and the shear strength of HSC. When the ductility number of the concrete coincided with that of the aggregate, the shear strength remained constant irrespective of concrete strength. However, when the ductility number of the concrete was higher than that of the aggregate, shear strength started to decrease due to the smooth fracture surface and brittleness. However, in this study, the maximum coarse aggregate size was 19 mm and the rock type was crushed granite. Therefore, further studies on different aggregate sizes and rock types are essential.

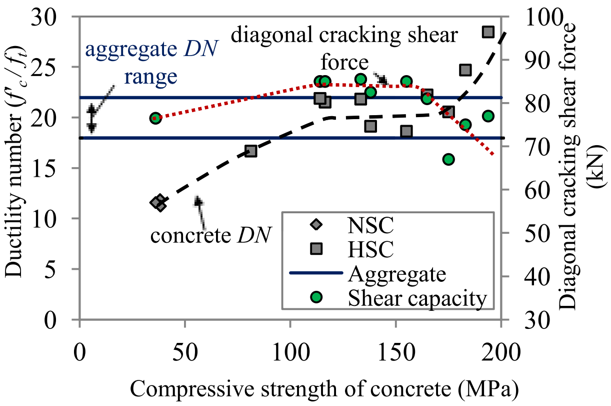

Fig.8 Effect of compressive strength of concrete on ductility number (*DN*) and diagonal cracking shear force of RC beams

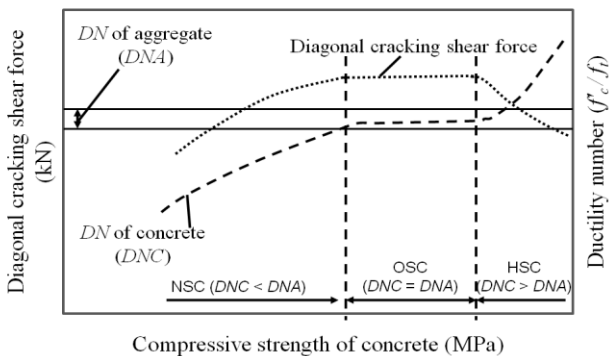

Fig.9 Effect of compressive strength of concrete on *DN* and diagonal cracking shear force of RC members (NSC: Normal strength concrete, OSC: Optimal strength concrete, HSC: High-strength concrete)

REFERENCES

1) Mutsuyoshi, H., Ichinomiya, T., Sakura, M., and Perera, S.V.T.J., "High-Strength Concrete for Prestressed Concrete Structures," Concrete Plant International, pp. 42-46, Aug. 2010.
2) Perera, S.V.T.J., and Mutsuyoshi, H., "Shear Behavior of Reinforced High-Strength Concrete Beams," ACI Structural Journal, Vol. 110-S05, pp. 43-52, Jan.-Feb. 2013.
3) Zararis, D.P., and Papadakis, G. C., "Diagonal Shear Failure and Size Effect in RC Beams without Web Reinforcement," Journal of Structural Engineering, ASCE, Vol. 127-7, pp. 733-742, 2001.
4) Perera, S.V.T.J., Mutsuyoshi, H., Takeda, R., and Asamoto, S., "Shear Behavior of High-Strength Concrete Beams," Proc. of Japan Concrete Institute, Vol. 32-2, Saitama-Japan, pp.685-690, 2010.
5) Taylor, R., and Brown, R.S., "The Effect of the Type of Aggregate on the Diagonal Cracking of Concrete Beams," Magazine of Concrete Research, July 1963.
6) Mehta, P.K., "Concrete: Structure, Properties, and Materials," Prentice-Hall, Inc., Englewood Cliffs, pp.36-40, 1986.
7) Aïtcin, P.-C., and Mehta, P.K., "Effect of Coarse-Aggregate Characteristics on Mechanical Properties of High-Strength Concrete," ACI Material Journal, Vol. 87-2, pp.103-107, March-April 1990.
8) Khuntia, M., and Stojadinovic, B., "Shear Strength of Reinforced Concrete Beams without Transverse Reinforcement," ACI Structural Journal, Vol. 98-5, pp.648-656, Sept-Oct. 2001.
9) Gettu, R., Bazant, Z.P., and Karr, M.E., "Fracture Properties and Brittleness of High-Strength Concrete," ACI Material Journal, Vol. 87-66, pp.608-618, Nov.-Dec. 1990.
10) Fairhurst, C., "On the Validity of the Brazilian Test for Brittle Materials," Int. J. Rock Mech. Mining Sci., Pergamon Press, Vol. 1, pp. 535-546, 1964.
11) Yagiz, S., "Assessment of Brittleness Using Rock Strength and Density with Punch Penetration Test," Tunnelling and Underground Space Technology, Vol. 24, pp. 66-74, 2009.
12) Gong, Q.M., and Zhao, J., "Influence of Rock Brittleness on TBM Penetration Rate in Singapore Granite," Tunnelling and Underground Space Technology, Vol. 22, pp. 317-324, 2007.
13) Přikryl, R., "Some Microstructural Aspects of Strength Variation in Rocks," International Journal of Rock Mechanics and Mining Sciences, Vol. 28, pp.671-682, 2001.
14) Franklin, J.A., and Dusseault, M.B., "Rock Engineering," McGraw-Hill, New York, pp. 237-267, 1989.
15) Fujita, M., Sato, R., Matsumoto, K., and Takaki, Y., "Size Effect on Shear Strength of RC Beams Using HSC without Shear Reinforcement," Translation from Proceeding of JSCE, Vol. 711 / V-56, pp.113-128, August 2002.
16) Sato, R., and Kawakane, H., "A New Concept for the Early Age Shrinkage Effect on Diagonal Cracking Strength of Reinforced HSC Beams," J. of ACT, Vol. 6, No. 1, pp.45-67, Feb. 2008.